Small-Molecule EGFR Inhibitor Induces DNA Damage and Disrupts EGFR-WEE1 Interaction in Glioblastoma

Jianzheng Huang[1], Zijun Zhang[1], Yang Xiao[1], Ziming Zhao[1], Zengwei Luo[1], Junjun Liu[1], Suitian Lai[1], Chao Song[2], Shouchang Feng[3], Suojun Zhang[3], Xingjiang Yu[2], Qingyi Tong[1*], Yonghui Zhang[1*]

[1]Department of Hubei Key Laboratory of Natural Medicinal Chemistry and Resource Evaluation, School of Pharmacy, Tongji Medical College, Huazhong University of Science and Technology, Wuhan, 430030, China;

[2]Department of Histology and Embryology, School of Basic Medicine, Tongji Medical College, Huazhong University of Science and Technology, Wuhan, China;

[3]Department of Neurosurgery, Tongji Hospital, Tongji Medical College, Huazhong University of Science and Technology, Wuhan, China.

Corresponding Author: Yonghui Zhang, Department of Hubei Key Laboratory of Natural Medicinal Chemistry and Resource Evaluation, School of Pharmacy, Tongji Medical College, Huazhong University of Science and Technology, 13 Hangkong Road, Jianghan District, Wuhan, Hubei Province, 430030, China (zhangyh@mails.tjmu.edu.cn.); Qingyi Tong, Department of Hubei Key Laboratory of Natural Medicinal Chemistry and Resource Evaluation, School of Pharmacy, Tongji Medical College, Huazhong University of Science and Technology, 13 Hangkong Road, Jianghan District, Wuhan, Hubei Province, 430030, China (qytong@hust.edu.cn.);

Abstract

Glioblastoma (GBM) is a highly aggressive primary brain malignancy with limited therapeutic options, underscoring the urgent need for novel therapeutic agents. Epidermal growth factor receptor (EGFR) remains a key therapeutic target due to its

critical role in tumor progression and therapy resistance. ZYH005 (Z5), a small molecule with low systemic toxicity and enhanced blood-brain barrier penetration, warrants further investigation for its therapeutic efficacy and mechanisms in GBM. Here, we demonstrate that Z5 exhibits potent anti-proliferative effects against conventional GBM cell lines and patient-derived glioblastoma stem cells (GSCs), while significantly suppressing GSCs-induced orthotopic tumor growth and prolonging survival in murine models. Through the mechanistic studies, we identify Z5 as a novel EGFR inhibitor that uniquely binds EGFR at E762 to induce DNA damage, subsequently impairing DNA repair mechanisms and disrupting EGFR-WEE1 interactions. This disruption suppresses WEE1 function, abrogates the G2/M checkpoint, and triggers mitotic catastrophe in GBM cells. Notably, we reveal a previously uncharacterized physical EGFR-WEE1 interaction in GBM, defining a new therapeutic axis. Structural analyses further suggest that the spatial orientation of E762 critically modulates EGFR-WEE1 complex formation. Collectively, these findings establish Z5 as a promising lead compound and provide a novel strategy for GBM drug development.

Key words: Glioblastoma; EGFR-WEE1 axis; mitotic catastrophe; DNA damage

Running title: Small molecule targets EGFR to disrupt EGFR-WEE1 axis in GBM.

1. Introduction

Glioblastoma multiforme (GBM) stands as the most invasive and deadly primary brain tumor among adults[1]. It constitutes around 49% of all malignant central nervous system tumors. In high-income countries, its annual incidence is 3-7 cases per 100,000 individuals[2,3]. The treatment of GBM adopts a multimodal strategy, integrating surgery, radiotherapy, and temozolomide (TMZ)-based chemotherapy. However, the median survival time for GBM patients is a mere 12-16 months, and the 5-year survival rate remains below 5%[2,3]. The unrelenting therapeutic deadlock in

neuro-oncology makes the development of novel drugs not just important, but an urgent medical necessity.

Epidermal growth factor receptor (EGFR) and its constitutively active mutant EGFRvIII are cardinal oncogenic drivers in GBM, with EGFR amplification present in more than 50% of tumors—predominantly the classical subtype[4]. This genetic alteration activates pro-tumorigenic cascades (PI3K/AKT/mTOR, RAS/MAPK, JAK/STAT), collectively driving genome instability, angiogenesis, and invasive growth[5]. In addition to activating downstream signaling pathways through ligand binding at the cell membrane, EGFR can also translocate into the nucleus, where it participates directly in DNA repair processes. Within the nucleus, EGFR forms functional interactions with DNA-dependent protein kinase catalytic subunit (DNA-PKcs), promoting its phosphorylation and thereby modulating DNA repair through the non-homologous end joining (NHEJ) pathway[6]. Beyond this direct mechanism, EGFR exerts broader control over DNA repair processes by regulating the expression of key repair proteins XRCC1 and RAD51 through the RAS/RAF/MEK/ERK and PI3K/AKT signaling cascades. These multifaceted EGFR-mediated adaptations collectively disrupt DNA damage response (DDR) homeostasis, creating a permissive environment for tumor cells to evade cell cycle checkpoints and survive genotoxic insults[7,8]. EGFR's central role in coordinating DNA repair explains why its pharmacological inhibition impairs DDR pathways, thereby sensitizing tumor cells to radiotherapy and other DNA-targeting therapies [9,10]. This has long established EGFR as a prime therapeutic target in GBM [11], while

highlighting the impact of EGFR inhibitors on DDR-related pathways and providing a mechanistic rationale for their combination with other agents, including DDR-targeted therapies[11]. For instance, although EGFR tyrosine kinase inhibitors (TKIs) demonstrate promising monotherapy efficacy, combination strategies—particularly pairing EGFR-TKIs with MEK/PI3K inhibitors or DNA-damaging agents (e.g., temozolomide, radiotherapy)—achieve superior outcomes by exploiting temporal vulnerabilities in DDR pathways. Preclinical studies further demonstrate that timed EGFR-TKI administration (≥4 hours before DNA damage induction) potentiates tumor cell killing by prolonging DDR pathway disruption [12,13]. Thus, EGFR remains a pivotal therapeutic target in GBM drug development due to its central pathogenic role and druggability[11,14,15].

Phenanthridinone, a key heterocyclic scaffold widely found in bioactive alkaloids, holds great potential for anti-tumor drug development[16,17]. Among its derivatives, narciclasine and related analogs exhibit the strongest anticancer effects[18-20]. However, their natural scarcity limits drug research. We developed an efficient, eco-friendly synthetic method for phenanthridone, enabling scalable derivative production and overcoming supply challenges[21].Using this approach, we designed and synthesized a series of phenanthridone derivatives, identifying ZYH005 (Z5) as the lead candidate with superior anticancer efficacy over narciclasine[22]. This finding prompts us to systematically investigate Z5's anti-tumor effects and molecular mechanisms, while also allowing us to draw insights from the preliminary studies on narciclasine. Narciclasine exhibits selective in vivo efficacy against primary GBM and

brain-metastatic melanoma/lung cancer[18,19], with efficient blood-brain barrier (BBB) penetration attributed to its high lipophilicity, positioning it as a promising GBM therapeutic[20]. Structurally, Z5 exhibits reduced hydrophilic (hydroxyl) groups, suggesting enhanced lipophilicity. In vivo BBB permeability assays in mice confirmed Z5's superior brain penetration compared to narciclasine (Supplementary Figures 1A-D). Given these pharmacokinetic advantages and structural optimizations, we hypothesized that Z5 may replicate or even exceed narciclasine's anti-GBM efficacy. Yet, the anti-GBM efficacy and mechanisms of this more potent phenanthridone derivative remain unexplored.

Here, we unveil Z5 as a novel EGFR inhibitor with potent anti-GBM activity—suppressing both bulk GBM cells and glioblastoma stem cells (GSCs) in vitro and in vivo. Our study breaks new ground by identifying Z5's mechanism: precise targeting of EGFR's E762 residue to trigger DNA damage, impair repair, and disrupt a previously unrecognized physical interaction between EGFR and WEE1. This disruption not only halts WEE1 function and abrogates the G2/M checkpoint but also drives catastrophic mitotic failure in GBM cells. By linking EGFR-WEE1 crosstalk to mitotic catastrophe, we uncover a novel therapeutic axis and position Z5 as a transformative lead compound for GBM treatment.

2. Materials and Methods

2.1 Compounds and cell lines

Z5 was synthesized in our laboratory, and its synthesis process has been described previously[22]. U87-MG (RRID: CVCL_0022), U251-MG (RRID: CVCL_0021) and

HEK293T (RRID: CVCL_0063) cell lines were purchased from Procell Life Science & Technology. DT40-related cell lines were gifts from Xiaohua Wu and Shunichi Takeda. GBM patient-derived GSCs (T3359 and D456) were gifted from Dr. Shideng Bao and Dr. Jeremy Rich[23]. U87-MG, U251-MG and HEK293T cells were cultured in DMEM (Pricella, Wuhan, China) supplemented with 10% Fetal Bovine Serum (FBS) and 1% penicillin/streptomycin. DT40 cells were cultured in 1640 with 10% FBS, 1% Chicken Serum, 1% penicillin/streptomycin, 1% 200mM L-Glutamine and 0.1% β-mercaptoethanol[24]. GSCs were cultured in a serum-free system containing Neurobasal A basal medium supplemented with B-27 Supplement Minus Vitamin A, l-glutamine, sodium pyruvate, 20 ng/ml recombinant epidermal growth factor, and 20 ng/ml basic fibroblast growth factor. Cell culturing, cryopreservation, and thawing were all meticulously conducted in strict accordance with standard operating procedures (SOPs). Short tandem repeat (STR) profiling and contamination assessment of the cell lines were performed every six months. The results verified the authenticity of the cell lines and confirmed their contamination-free status.

2.2 DNA Microarrays and Gene Set Enrichment Analysis (GSEA) analysis

Total RNA samples were extracted from U87-MG cells using the Trizol reagent (Cat#15596-018, Life Technologies, Carlsbad, CA, US) reagent. RNA purification was performed using the NucleoSpin RNA Clean-up XS kit (Cat#740903, MN, Germany) and the RNase-Free DNase Set (Cat#79254, QIAGEN, GmBH, Germany). According to the Affymetrix technical manual, the double-stranded cDNA was

hybridized with biotin-labeled fragmented cRNA. Microarray experiments were performed using Affymetrix chips by Shanghai Biotechnology Corporation. Raw data were normalized using the Expression Console algorithm in Command Console Software 4.0 (Affymetrix, Santa Clara, CA, US). Differential expression analysis was conducted using the affy package in R. Genes with an absolute log2 fold change >1 and a P-value <0.05 were considered differentially expressed. The microarray data for U87-MG cells has been submitted to the NGDC/OMIX under accession number OMIX008765. Significantly differentially expressed genes ($|Log2FC| \geq 1$, $FDR \leq 0.05$) are listed in **Supplementary Table S1**. All genes identified through DNA microarray analysis were imported into GSEA software for further analysis and visualization.

2.3 Connectivity map (CMAP) analysis

Input the top 66 upregulated genes and 150 downregulated genes in supplementary S1 into the CMAP website (https://clue.io), query parameters were gene expression (L1000), touchstone, individual query, 1.0. The detailed list was sorted by cell types and perturbagen type was compound. The results obtained from CMAP are presented in **Supplementary Tables S2-S11**.

2.4 Molecular Docking of Z5 with the EGFR Kinase Domain

For our molecular docking, we utilized the crystal structure of EGFR (PDB ID 7KXZ)[25]. This structure was preprocessed using PDB2PQR program[26] to determine the protonation state of titratable residues at pH=7, and was subsequently converted to

pdbqt format using the prepare_receptor4.py script from AutoDockTools[27]. Next, we prepared ZYH005 by converting compounds to pdbqt format (pH 7.0) using OpenBabel. Using molecular docking scores as an indicator of predicted binding affinity.

2.5 Limited Proteolysis–Mass Spectrometry (LiP-MS)

LiP-MS was performed as previously published[28]. A detailed description is in **Supplementary Material**.

2.6 Tissue Microarray and Immunohistochemistry

Tissue microarrays were obtained from Wuhan POWERFUL BIOLOGY Company and approved by the Ethics Committee of Tongji Hospital of Tongji Medical College of Huazhong University of Science and Technology (Serial number: 2021-lEC-A244). The GBM tissue samples for TMA were prepared by dewaxing and antigen retrieval prior to immunostaining. WEE1 antibody (Cell signaling technology, 1:200 dilution) was used to detect the protein in the GBM tissue samples. IHC for in situ transplanted mouse brain tissues was carried out using the same protocol as described above. WEE1 antibody (Cell signaling technology, 1:200 dilution) and EGFR antibody (Proteintech, 1:100 dilution) were used to detect the protein.

2.7 Orthotopic Transplantation mouse model assay

Experimental Balb/c nude mice were purchased from Beijing Vital River Laboratory

Animal Technology Co., Ltd (Beijing, China) and kept at the Experimental Animal Center of Tongji Medical College, Huazhong University of Science and Technology, Wuhan, China. All mice underwent phenobarbital sodium anesthesia before surgery. One week after GSC ($2x10^4$ cells/mouse) was implanted in the right frontal lobe of 4-week-old mice, 15 mice were randomly divided into three groups: NT, Z5-L (10mg/kg) and Z5-H (20mg/kg). The mice received either solvent (5% DMSO, 20% castor oil, and 75% saline) or varying doses of the drug via gavage for 7 weeks. When the NT group showed the first manifestation of obvious neurological signs, one mouse from each of the remaining two groups was evaluated for drug efficacy. The remaining 12 mice were used for survival studies.

2.8 Statistical analysis

Statistical analysis was performed using GraphPad Prism 9.0 software. The data were expressed as the mean ± SD. We used paired t test for statistical analysis between 2 groups, and one-way ANOVA for multiple comparisons. All experiments were repeated more than 3 times. We considered a p-value less than 0.05 to be statistically significant.

3. Results

3.1 Z5 inhibits the proliferation and induces DNA damage in GBM cells

Quantitative viability assays demonstrated that Z5 potently inhibited GBM cell proliferation in a time- and concentration-dependent manner, with 72-hour IC50

values of 0.114 ± 0.016 μM for U87-MG cells and 0.147 ± 0.049 μM for U251-MG cells (Figure 1A). Z5 also significantly suppressed colony formation in both cell lines (Figure 1B), while EdU incorporation assays further confirmed its marked inhibition of DNA synthesis (Figures 1C-D). These anti-proliferative effects coincided with clear evidence of DNA damage induction, as shown by increased DNA fragmentation (Figure 1E) and elevated γ-H2AX expression—a sensitive marker of double-strand breaks (Figure 1F)—consistent with Z5's established mechanism as a DNA intercalator[22]. Collectively, these findings establish Z5 as a potent cytotoxic agent against GBM cells that mediates its effects through robust inhibition of proliferation and induction of DNA damage.

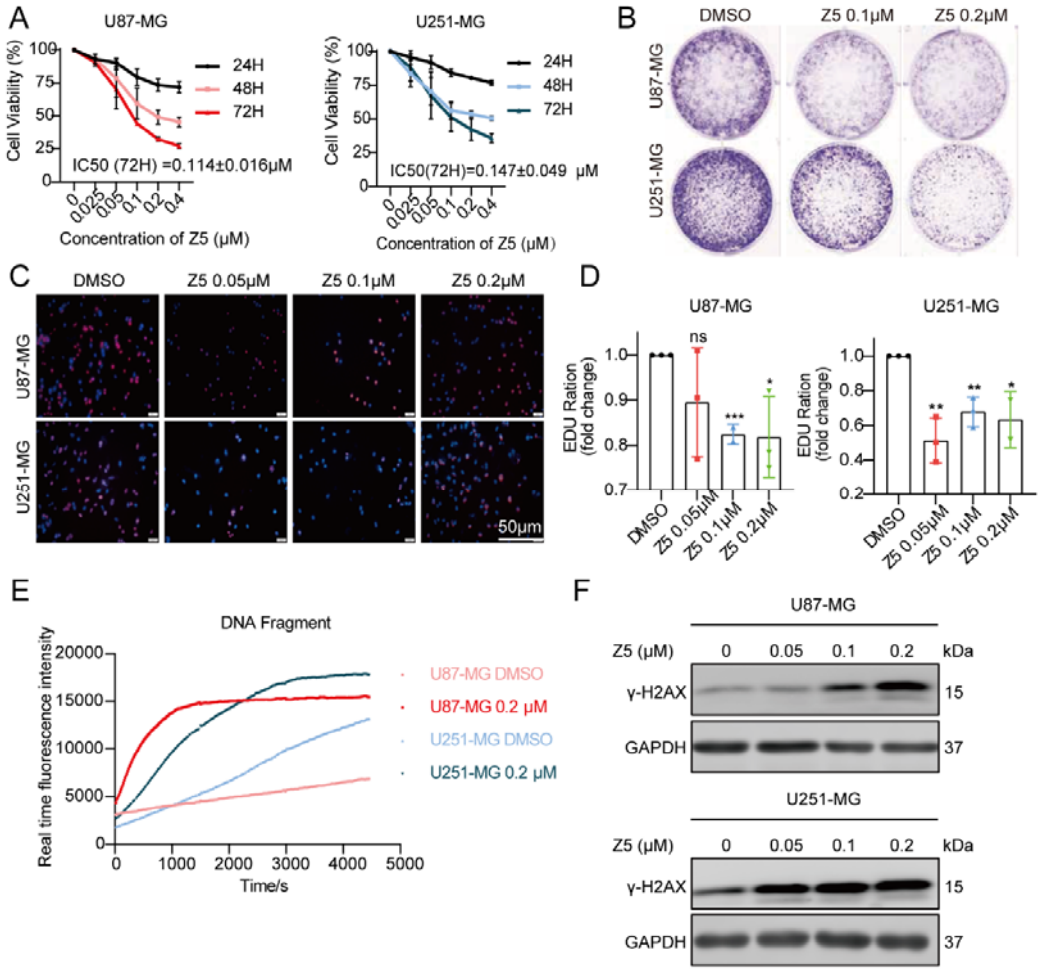

Figure 1 Z5 inhibits the proliferation and induces DNA damage in GBM cells. (A) Cell viability was evaluated using CCK-8 kit after treated with Z5 for 24h, 48h and 72h. (B) The efficacy of Z5 in a colony formation assay was evaluated. (C) Fluorescent images of proliferating GBM cell lines in various treatment conditions (red: EDU staining; blue: Hoechst staining). (D) Quantification of the fluorescence of each group. Data are presented as the mean ± SD, n=3, compared with DMSO group. (E) Effect of Z5 on DNA fragment. (F) The expression of γ-H2AX was measured by immunoblotting after treatment with Z5.

3.2 Z5 induces G2/M arrest and mitotic catastrophe in GBM cells

To elucidate the molecular mechanisms underlying Z5's anti-GBM effects, we conducted a comprehensive microarray analysis, which identified 1,970 differentially expressed genes (188 upregulated and 1,782 downregulated) in Z5-treated U87-MG cells (Supplementary Figure 2A), with KPNA2, PRKDC, and MKI67 being the most significantly downregulated targets (Supplementary Figures 2B-C).

Subsequent KEGG, GO, and GSEA enrichment analyses revealed that Z5 predominantly affects cell cycle and mitotic cell cycle pathways (Figures 2A-B), with GSEA specifically highlighting its involvement in G2/M phase transition, checkpoint control, and mitotic spindle function (Figure 2C). Notably, transcriptional analysis showed significant downregulation of WEE1 (≈67%) and CDK1 (≈55%), key regulators of the G2/M checkpoint where WEE1 governs CDK1 phosphorylation to control mitotic entry. This was further validated by flow cytometry demonstrating increased G2/M phase accumulation and PHH3 positivity (Figure 2D), coupled with reduced WEE1 and CDC2 phosphorylation alongside elevated phospho-histone H3 levels following Z5 treatment (Figure 2E), collectively indicating G2/M checkpoint disruption.

Subcellular localization analysis (GOCC and GSEA) indicated that Z5 predominantly accumulates in nuclear compartments, replication forks, and chromosomal regions (Figure 2B, Supplementary Figure 2D), consistent with its DNA intercalation properties. Since DNA damage typically triggers the DDR, leading to WEE1-mediated G2/M arrest to facilitate repair, we investigated whether Z5 impairs

this protective mechanism. Strikingly, GSEA revealed significant suppression of DNA repair pathways (Supplementary Figure 2E). To validate this, by adopting the well-known DT40-DDR research model[24], we found that the knockdown of key genes involved in DNA repair (e.g., Rev3 in TLR) increased the efficacy of Z5 (Supplementary Figure 2F). These findings suggest that inhibition of DNA repair pathways may play a facilitative role in enhancing Z5's functional activity. Finally, immunofluorescence microscopy revealed characteristic mitotic catastrophe features including chromosomal missegregation, multipolar spindle formation, and micronucleation (Figure 2F). Collectively, these findings demonstrate that Z5 induces DNA damage while simultaneously disrupting DNA repair mechanisms and G2/M checkpoint control, ultimately triggering lethal mitotic catastrophe in GBM cells.

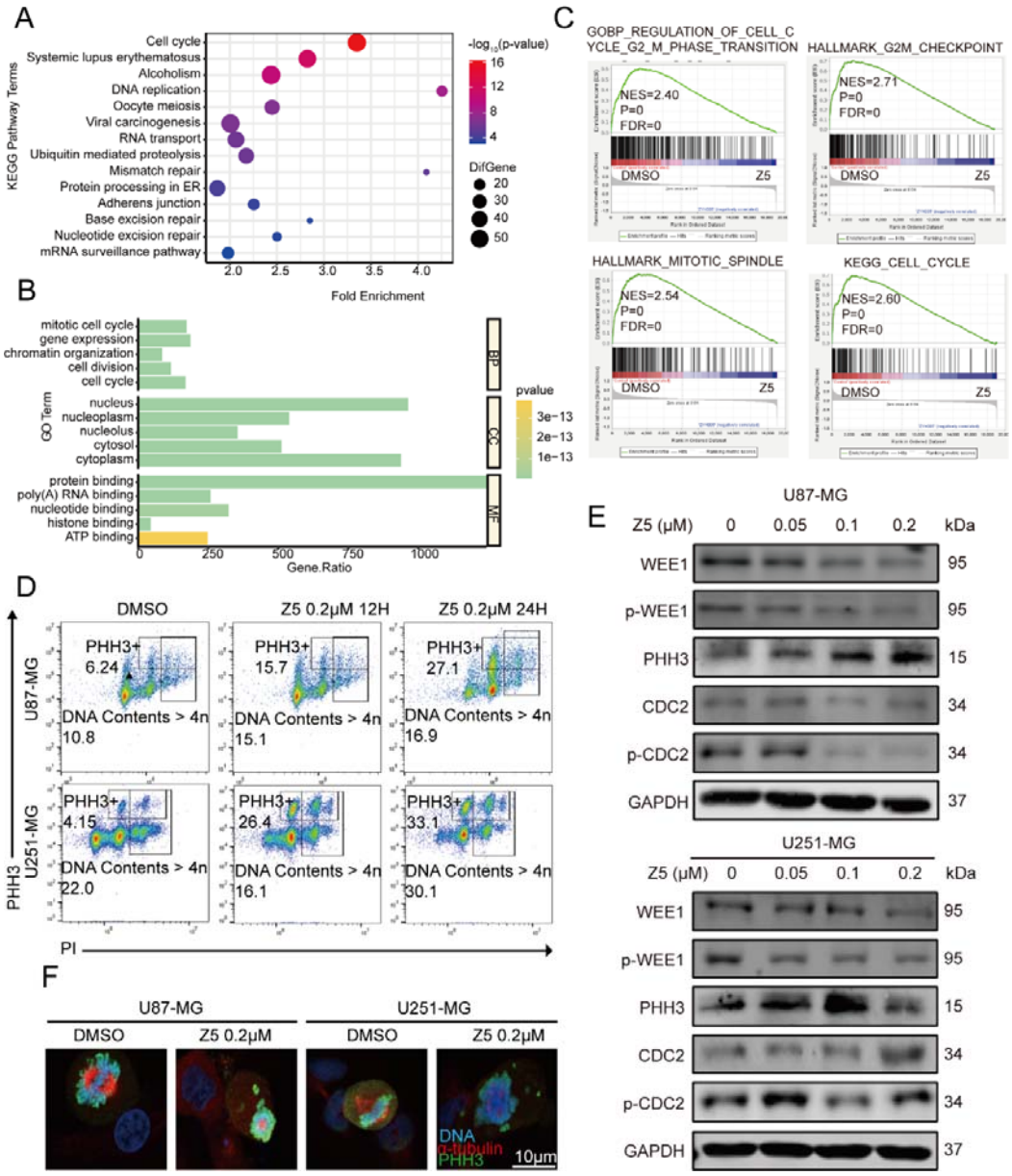

Figure 2 Z5 induces G2/M arrest and mitotic catastrophe in GBM cells. (A) KEGG pathway enrichment analysis and (B)GO enrichment analysis of downregulated genes identified by the U87-MG microarray. ER: Endoplasmic Reticulum. (C) GSEA analysis of Cell cycle of G2/M phase transition, G2M checkpoint, mitotic spindle and cell cycle pathways. (D) Representative flow cytometric analysis of PHH3+ and DNA contents > 4n cells. (E) The expressions of

WEE1, p-WEE1, PHH3, CDC2, p-CDC2 in GBM cells were measured by immunoblotting after treatment with different concentrations of Z5 for 48h. (F) Immunofluorescence staining was performed with anti-tubulin (Red), anti-PHH3 (Green) on the U87-MG and U251-MG cells treated with or without Z5.

3.3 Z5 targets EGFR

To elucidate Z5's mechanism of action, we employed the Connectivity Map (CMAP), a computational drug repurposing tool that identifies functional connections between drugs, genes, and diseases by comparing gene expression signatures [29].

Querying CMAP with a signature comprising the top 66 upregulated and top 150 downregulated genes from our microarray data yielded positive connectivity scores for multiple compounds. Data were categorized by cell type, selecting only compound perturbagens, and the top 10 compounds per cell type were identified based on ranking. Statistical analysis revealed EGFR inhibitors as the most frequent functional matches (Supplementary Tables 2-11, Figure 3A). This computational prediction was further supported by GSEA analysis showing Z5-mediated inhibition of the PI3K/AKT/mTOR pathway and mTORC1 activation (Supplementary Figure 2E), which are well-established pharmacological effects of EGFR inhibitors.

Based on these findings, we hypothesized that Z5 might directly target EGFR. To test this, we performed a series of biochemical assays. Cellular thermal shift assay (CETSA) demonstrated that Z5 enhanced the thermal stability of EGFR in both U87-MG and U251-MG cells (Figure 3B), while drug affinity responsive target

stability (DARTS) assays showed that Z5 protected EGFR from proteolytic degradation (Figure 3C). Most conclusively, surface plasmon resonance (SPR) experiments confirmed direct binding between Z5 and the EGFR kinase domain with a dissociation constant (KD) of 19.6 μM (Figure 3D). Functional studies revealed that Z5 treatment significantly reduced phosphorylation of EGFR (p-EGFR), ERK (p-ERK), and mTOR (p-mTOR) in both cell lines, while unexpectedly increasing total EGFR levels in U251-MG cells (Figure 3E).

To substantiate the interaction between Z5 and EGFR, we evaluated the impact of EGFR silencing on Z5-induced antiproliferative effects. We first assessed the knockdown efficiency of EGFR-targeting siRNAs in GBM cell lines, selecting siEGFR-1261 for subsequent experiments based on its superior efficacy (Supplementary Figure 3A). Our results demonstrated that siRNA-mediated EGFR knockdown significantly weakened Z5's proliferative inhibition in both CCK8 and EdU assays (Figures 3F-G). Furthermore, EGFR silencing abolished Z5-induced G2/M arrest and suppressed the upregulation of γ-H2AX and PHH3 proteins (Figures 3H-I). Collectively, these data demonstrate that Z5 exerts its anti-GBM effects through direct EGFR inhibition, leading to disrupted downstream signaling and ultimately inducing cell cycle arrest and DNA damage responses.

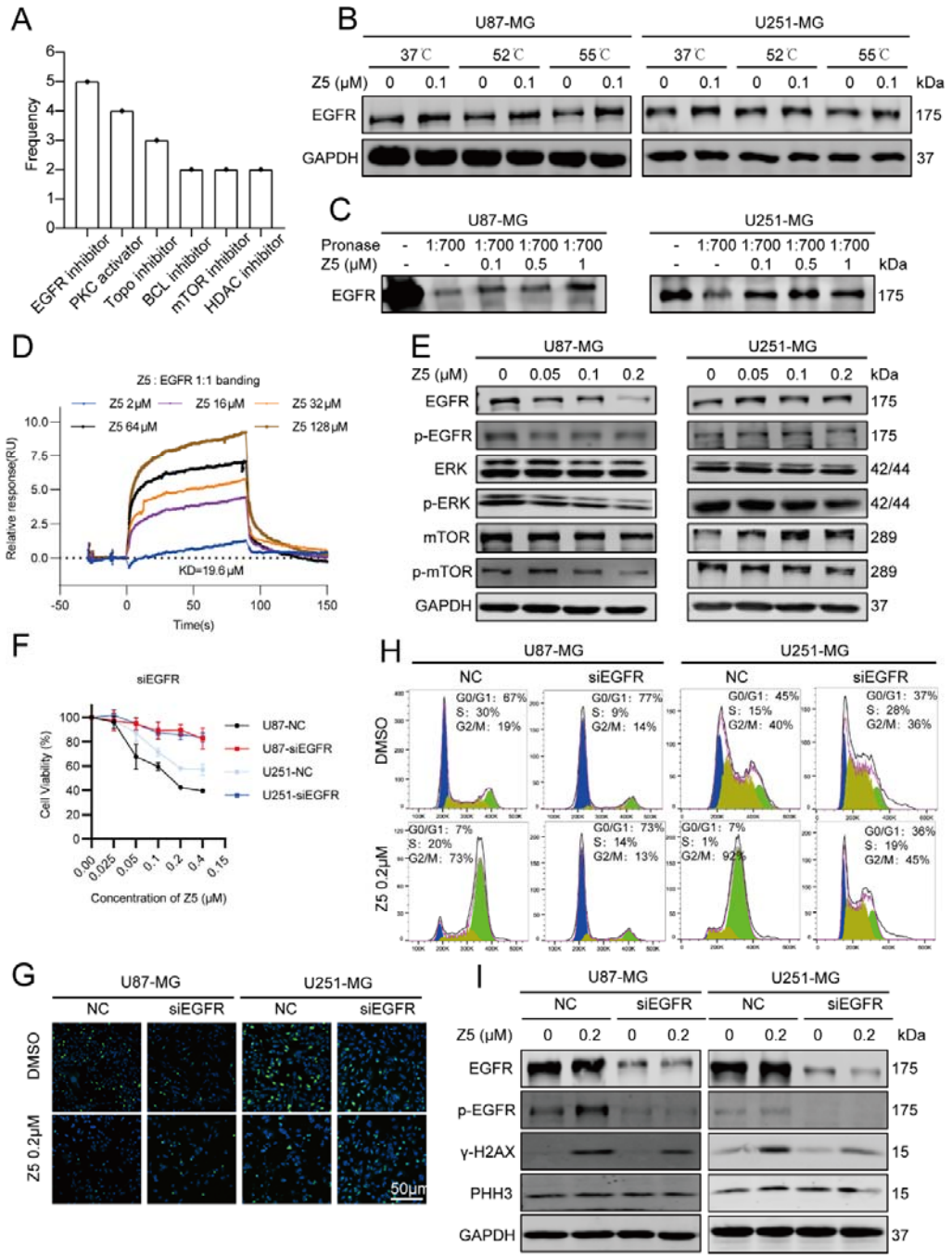

Figure 3 Z5 targets EGFR. (A) In the CMAP data, the top 10 compounds positively correlated with microarray data were selected for each cell type. The descriptions of these compounds were then statistically analyzed, and the descriptions were ranked

based on their frequency of occurrence. (B) The CETSA assay was used to evaluate the binding between Z5 (0.1mM) in thermodynamic levels. The expression of EGFR was detected by immunoblotting. (C) The DARTS assay was used to evaluate the binding between different concentrations of Z5. The expression of EGFR was detected by immunoblotting. (D) Interaction between Z5 and recombinant EGFR kinase domain protein was analyzed by SPR. (E) The expression of EGFR, p-EGFR, ERK, p-ERK, mTOR, p-mTOR in U87-MG and U251-MG cells were measured by immunoblotting after treatment with different concentrations of Z5 for 48h. (F) Growth curves of GBM cell lines transfected with or without si-EGFR and treated with or without Z5 for 48H. (G) The efficacy of Z5 on GBM cell lines transfected with or without si-EGFR was detected by EDU staining. (H) The cell cycle of GBM cell lines transfected with or without si-EGFR was evaluated using flow cytometry after being treated with or without Z5 for 24h. (I) The expression of EGFR, p-EGFR, γ-H2AX and PHH3 in U87-MG and U251-MG cells were measured by immunoblotting after treatment with Z5 for 48h.

3.4 Z5 binds to the E762 residue of EGFR

To elucidate the structural basis of Z5-EGFR binding, we conducted comprehensive molecular docking simulations targeting the ATP-binding pocket of the EGFR kinase domain (PDB: 7KXZ). A detailed analysis of Z5's binding mode revealed key molecular interactions with EGFR: (1) extensive hydrophobic contacts with residues V702, L820, and L694, which stabilize its position within the ATP-binding pocket;

and (2) two critical hydrogen bonds formed with K721 and T766, likely contributing to its high binding affinity (Figure 4A).

To experimentally validate these computational predictions, we employed limited proteolysis-mass spectrometry (LiP-MS), a label-free proteomics approach, to map potential Z5 binding sites within the EGFR kinase domain. The LiP-MS results identified several peptide segments within the EGFR kinase domain that may serve as Z5 binding sites (Figures 4B-C). Notably, while the previously identified K721 and T766 residues from the docking studies were not directly detected by LiP-MS, we observed that K721 forms a hydrogen bond with E738, which may stabilize K721 and indirectly maintain the hydrogen bond interaction with Z5. By integrating these findings, we identified E738 (UniProt P00533-1 numbering: E762) as a critical binding site for Z5.

To functionally validate the importance of E762, we established an ectopic expression system in HEK293T cells transfected with either empty vector, wild-type (WT) EGFR, or the E762V mutant EGFR (Figure 4D). Dose-response experiments using CCK-8 assays demonstrated that Z5's antiproliferative effect reached a plateau at concentrations >0.1 μM, with residual viability stabilizing around 75% (Figure 4E). Based on these results, we selected 0.2 μM Z5 for subsequent experiments to ensure measurable effects while avoiding complete cytotoxicity.

Functional validation using both CCK-8 and EdU assays revealed that the E762V mutation significantly attenuated Z5’s therapeutic effect (Figures 4F-G). Compared to cells expressing WT-EGFR, those expressing the E762V mutant exhibited markedly

higher cell viability and proliferative capacity following Z5 treatment. These findings conclusively establish E762 as a key binding residue for Z5 on EGFR, essential for mediating its biological activity.

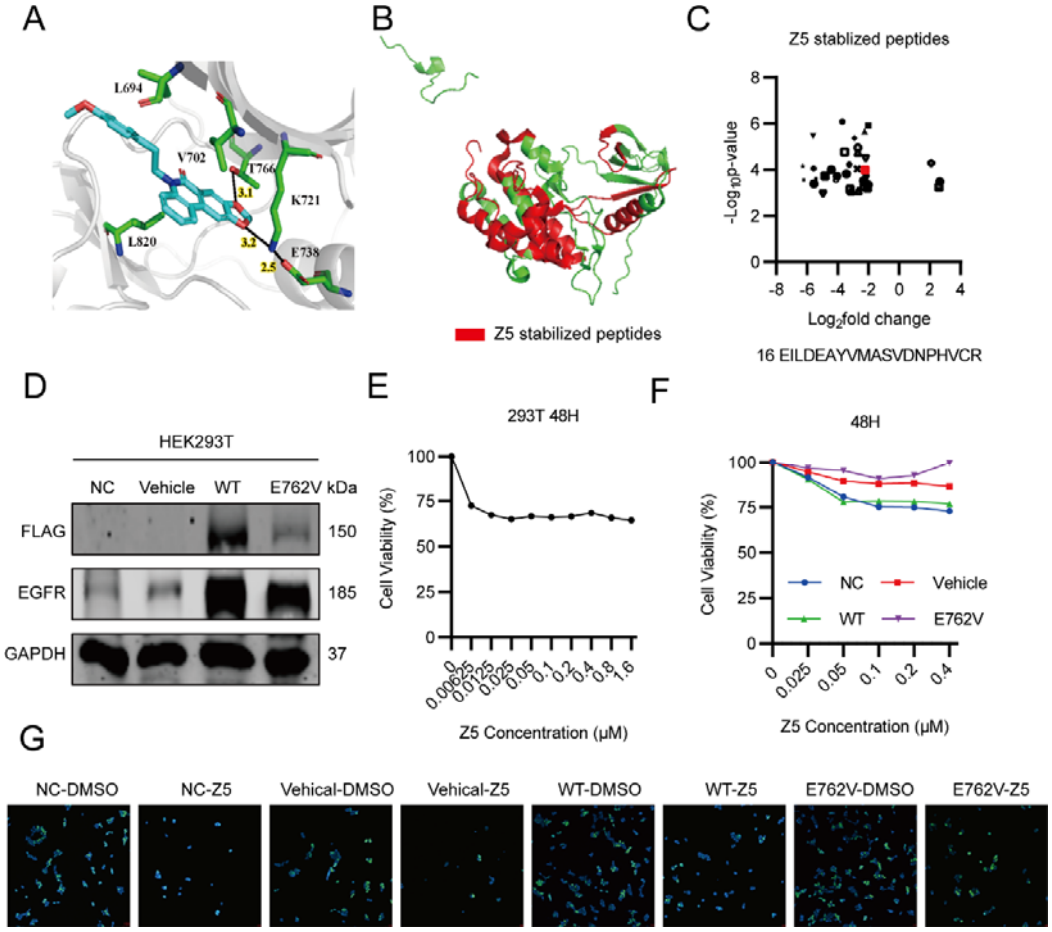

Figure 4 Z5 binds to the E762 residue of EGFR. (A) Binding mode of ZYH005 in EGFR kinase domain. Protein residues and ZYH005 are shown as sticks. Carbon atoms in ZYH005 are cyan, and those in protein residues are green. Oxygen and nitrogen atoms are rendered in red and blue, respectively. Black dashed lines indicate hydrogen bonds, with distances labeled in angstroms with yellow background. (B) Red regions indicate unstable peptides after Z5 treatment. Selection criteria: Log2(Fold change) > 2, -Log10(P-value) > 2. (C) Scatter plot showing peptides

identified by Lip-MS. Purified EGFR kinase domain protein was treated with 100 μM Z5 at room temperature for 15 minutes, followed by Lip-MS analysis. The scatter plot displays peptide abundance changes between the Z5-treated and control groups. X-axis shows Log2 (Fold change), Y-axis shows -Log10(P-value). (D) The expression of Flag and EGFR in HEK293T cell lines were measured by immunoblotting after transfected with different plasmids. (E) Growth curves of HEK293T cell lines treated with or without Z5 for 48H. (F) Cell viability was evaluated using CCK-8 kit after treated with Z5 for 48h. (G) Fluorescent images of proliferating GBM cell lines in various treatment conditions (green: EDU staining; blue: Hoechst staining).

3.5 WEE1 Overexpression Links to Aggressive GBM and EGFR Interaction

Our previous findings indicated that Z5 targets EGFR and suppresses WEE1-mediated G2/M phase arrest, thereby promoting entry into mitosis. Furthermore, knockdown of EGFR abrogated the cell cycle regulatory effects of Z5, suggesting that Z5's inhibition of WEE1 may occur via an EGFR-dependent mechanism. Through systematic bioinformatics analysis of the Chinese Glioma Genome Atlas (CGGA) database, we identified WEE1 as a particularly important player in GBM compared to other glioma subtypes (Supplementary Figure 4A). Notably, WEE1 expression showed significant variation among GBM molecular subtypes, with the Classical and Mesenchymal subtypes exhibiting markedly higher expression than the Proneural subtype (Supplementary Figure 4B). Furthermore, IDH-wildtype GBMs demonstrated significantly elevated WEE1 levels compared to their IDH-mutant counterparts (Supplementary Figure 4C), suggesting a potential link between WEE1 overexpression and the more aggressive GBM phenotype. Comprehensive survival

analyses utilizing both The Cancer Genome Atlas (TCGA) and the CGGA databases revealed a significant association between elevated WEE1 expression and adverse clinical outcomes, including reduced overall survival (OS) in GBM patient (Figure 5A; Supplementary Figures 4D–E). In summary, our data has uncovered the critical role of WEE1 in GBM and established its significant prognostic value in this aggressive malignancy.

To validate these findings at the protein level, we performed immunohistochemical analysis of WEE1 expression in a tissue microarray comprising 64 primary GBM samples representing all pathological grades (0-IV) and covering diverse brain regions. Our results demonstrated a clear positive correlation between WEE1 staining intensity and tumor grade (Figures 5B-C), further supporting WEE1's involvement in GBM progression.

Next, we investigated the relationship between WEE1 and EGFR. Bioinformatic analysis of the CGGA cohort demonstrated a statistically significant positive correlation between WEE1 and EGFR mRNA expression levels (Pearson’s R = 0.38) (Figure 5D). To validate these findings at the protein level, we performed immunofluorescence staining of GBM tumor tissues, which revealed distinct co-localization of EGFR and WEE1 proteins, supporting a potential functional interaction between these two molecules in GBM cells (Figure 5E). These findings provide strong evidence for a functional interaction between EGFR signaling and WEE1-mediated cell cycle regulation in GBM, offering a mechanistic explanation for our observation that Z5's effects on WEE1 are EGFR-dependent.

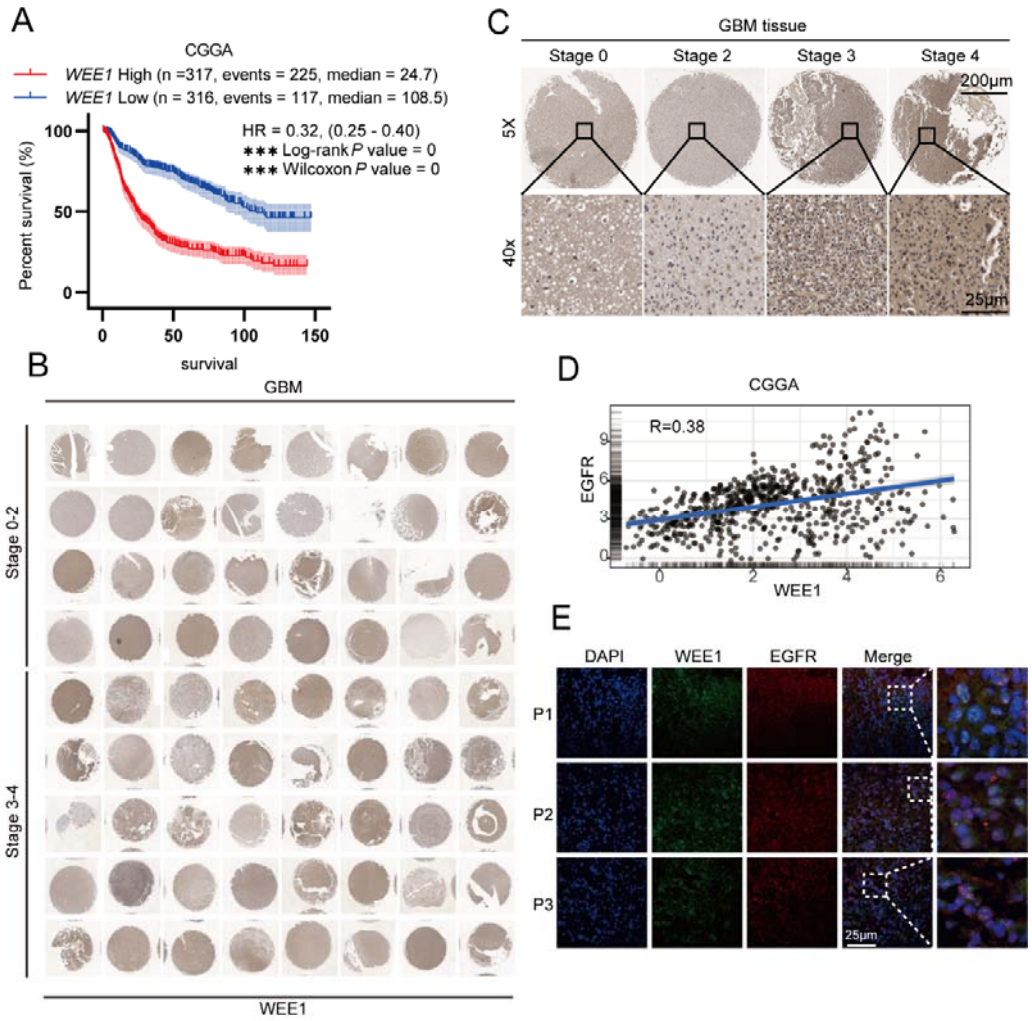

Figure 5 High Expression of WEE1 Is Correlated with Poor Prognosis in Patients and Positively Associated with EGFR Expression. (A) Association Between WEE1 Expression and Survival Time in CGGA Database. (B) TMA of GBM. (C) Representative images of WEE1 immunohistochemistry on the TMA are shown (original magnification: upper: 5x; lower: 40x). (D) Relationship between EGFR and WEE1 in GBM patients. (E) IF staining images of tumor tissues from GBM patients.

The ethical approval number: 2021-lEC-A244

3.6 Z5 inhibits EGFR to disrupt the EGFR-WEE1 axis

Our comprehensive mechanistic studies reveal a novel EGFR-WEE1 signaling axis

that serves as a critical therapeutic target in GBM. To quantitatively characterize the interaction between WEE1 and EGFR, we performed SPR analysis, which demonstrated a high-affinity binding between the kinase domains of WEE1 and EGFR, with an equilibrium dissociation constant (KD) of 17.3 nM (Figure 6A). This physical interaction was further confirmed by multiple experimental approaches: immunofluorescence microscopy demonstrated partial nuclear co-localization of EGFR with predominantly nuclear WEE1 (Figure 6B, Supplementary Figure 5A), while co-immunoprecipitation assays verified their endogenous interaction in GBM cells (Figure 6C, Supplementary Figure 5B). Strikingly, Z5 treatment induced dramatic subcellular redistribution of both proteins - causing WEE1 nuclear export while promoting EGFR nuclear accumulation - and significantly disrupted their physical association (Figures 6B-C, Supplementary Figures 5A-B).

The above findings reveal a direct interaction between EGFR and WEE1. This interaction is specifically inhibited by Z5, which targets residue E762 within the EGFR kinase domain. To understand the potential role of E762 in EGFR-WEE1 interaction, existing EGFR crystal structures were analyzed. Two distinct conformations of E762 were found in these structures: an inward-facing orientation towards the protein core (e.g., in PDB 4WKQ) and an outward-facing orientation (e.g., in PDB 6JXT) (Supplementary Figure 6A). We hypothesized that the solvent-exposed (outward-facing) conformation of E762 is required for EGFR-WEE1 binding, because only the residues in protein surface can take part in the protein-protein interaction. To test this hypothesis, two EGFR inhibitors, Gefitinib and AZD9291, were selected to test their activity toward EGFR-WEE1 interaction inhibition. Based on the crystal structures, Gefitinib and AZD9291 can stabilize E762 in the inward-facing and outward-facing conformations, respectively. We predicted that the former inhibitor

would disrupt the EGFR-WEE1 interaction, whereas the latter would not. Surprisingly, we found that Gefitinib disrupted the interaction between EGFR and WEE1, whereas AZD9291 enhanced their binding, as revealed by Co-IP (Supplementary Figure 6B). These results validate our hypothesis that an inward-oriented E762 conformation impairs the ability of EGFR to interact with WEE1.Therefore, we propose that Z5 exerts its inhibitory effect on the EGFR-WEE1 interaction by the same mechanism. It can induce or stabilize the inward-facing conformation of E762, thereby preventing the binding between EGFR and WEE1.

To further validate this signaling axis, we performed genetic and pharmacological interventions in U87-MG cells. While WEE1 silencing had no effect on EGFR expression or phosphorylation (p-EGFR), EGFR knockdown significantly reduced both WEE1 expression and its activating phosphorylation (p-WEE1) (Figure 6D). Pharmacological validation using targeted inhibitors yielded consistent results: MK1775 (WEE1 inhibitor) minimally affected EGFR signaling (p-ERK and p-mTOR), whereas AZD9291 (EGFR inhibitor) potently suppressed both WEE1 phosphorylation and CDC2 activation (p-CDC2) (Figure 6E). These findings establish EGFR as an upstream regulator of WEE1, defining a unidirectional signaling axis with functional crosstalk between these kinases.

Given that WEE1 acts downstream of EGFR and Z5 disrupts their interaction, we hypothesized that WEE1 knockdown would attenuate Z5’s therapeutic effects. siRNA-mediated WEE1 knockdown (siWEE1-1409, Supplementary Figure 3B) significantly reduced Z5's proliferative inhibition in both CCK8 and EdU assays (Figures 6F-G, Supplementary Figures 7A-B), abolished Z5-induced G2/M arrest (Figure 6H, Supplementary Figure 7C), and diminished Z5-mediated upregulation of γ-H2AX and PHH3 (Figure 6I, Supplementary Figure 7D). These results conclusively

demonstrate that Z5 exerts its anti-GBM effects through targeted disruption of the EGFR-WEE1 signaling axis.

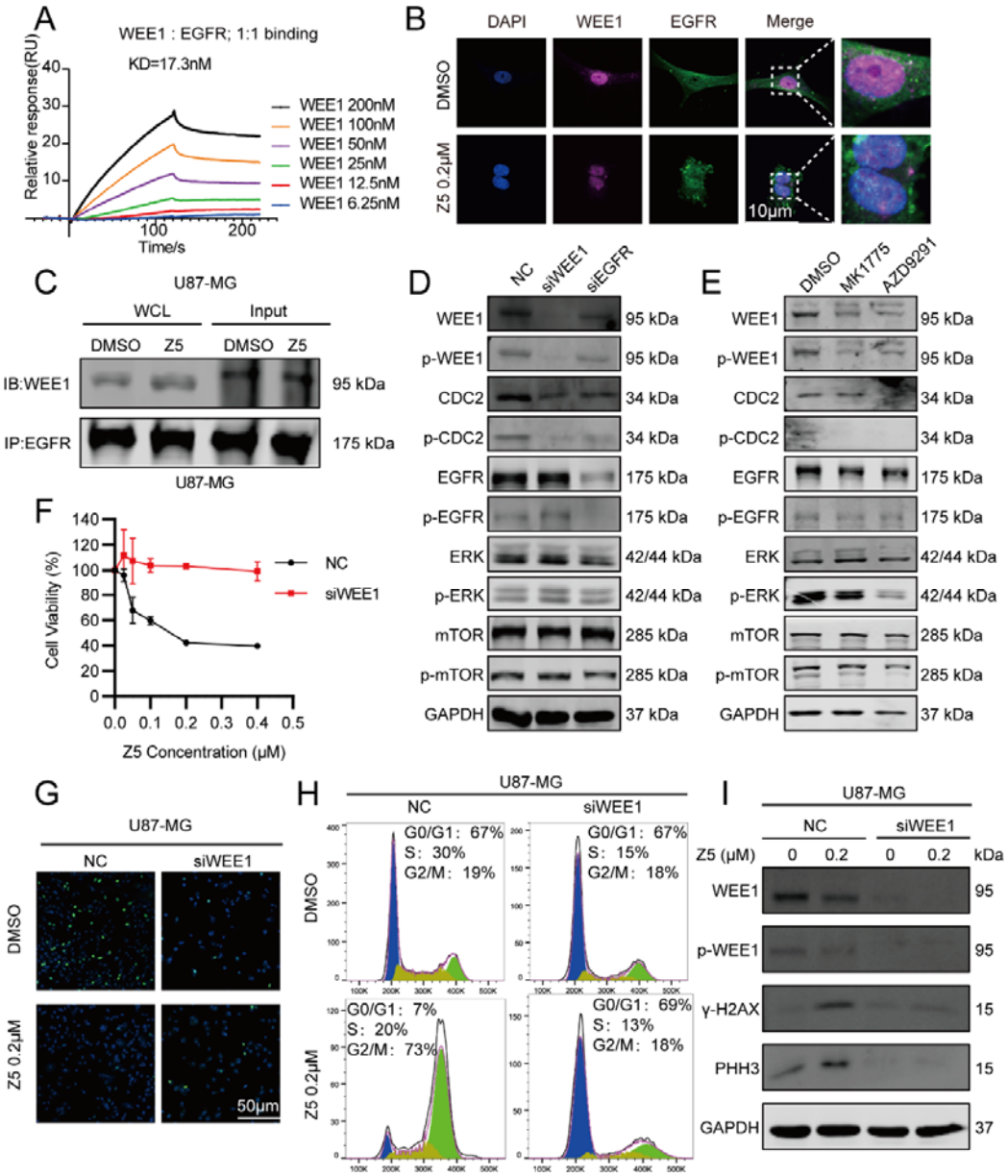

Figure 6 Z5 inhibits EGFR to disrupt the EGFR-WEE1 axis. (A) SPR analysis of the interaction between the kinase domains of EGFR and WEE1. (B) Confocal immunofluorescence staining was used to analyze the localization of EGFR and WEE1 in U87-MG cells. (C) Co-IP was used to detect the interaction between EGFR

and WEE1 after 15 min or untreated Z5 treatment in U87-MG cells. (D)Western blot analysis of WEE1, p-WEE1, CDC2, p-CDC2, EGFR, p-EGFR, ERK, p-ERK, mTOR, and p-mTOR expression levels following WEE1 or EGFR knockdown, (E)or treatment with MK1775 (4 μM) and AZD9291 (8 μM) in U87-MG cells. (F) Growth curves of U87-MG cell lines transfected with or without si-WEE1 and treated with or without Z5 for 48H. (G) The efficacy of Z5 on U87-MG cell lines transfected with or without si-WEE1 was detected by EDU staining. (H) The cell cycle of U87-MG cell lines transfected with or without si-WEE1 was evaluated using flow cytometry after being treated with Z5 for 24h. (I) The expression of WEE1, p-WEE1, γ-H2AX and PHH3 in U87-MG cells were measured by immunoblotting after treatment with Z5 for 48h.

3.7 Z5 inhibits GSCs tumorigenesis and progression through EGFR-WEE1 axis disruption

GSCs constitute a distinct subpopulation within glioblastoma, characterized by their stem-like properties and heightened capacity for DNA repair, which confers them with an increased resistance to chemotherapy drugs[30,31]. To investigate the efficacy of Z5 in vivo, we first tested its effects in two cell lines of patient-derived GSCs. Under microscopic examination, it became clear that Z5 exerted a substantial effect in inducing the fragmentation of tumor spheres formed by both 3359 and 456 GSCs lines (Figure 7A-B, Supplementary Figures 8A-B). Immunoblot analysis confirmed that Z5 significantly suppressed the EGFR-WEE1 signaling axis in both GSC lines (Figure 7C, Supplementary Figure 8C).

For in vivo validation, we selected the 3359 GSC line to establish an orthotopic

xenograft model in mice. When the first untreated (NT) mouse exhibited terminal symptoms, one mouse from each treatment group was euthanized for histological analysis. Hematoxylin and eosin (HE) staining demonstrated that Z5 treatment significantly inhibited GSC tumor growth in the brain (Figure 7D).

Moreover, Z5 notably prolonged the survival of model mice in a dose-dependent manner. The mean survival time of the mice in the control group was determined to be 102.75 days. For the Z5 - treated groups administered with dosages of 10 mg/kg and 20 mg/kg, the mean survival times of the mice reached 127.5 days and 139 days, representing increases of 24.1% and 35.3% relative to that of the control group, respectively (Figure 7E). IHC staining also demonstrated a significant reduction in EGFR and WEE1 expression within tumors following Z5 treatment (Figure 6F, Supplementary Figures 8D-E). Furthermore, following 8 weeks of Z5 treatment, the results of HE staining showed no signs of toxicity in the heart, liver, spleen, lungs, and kidneys of the mice (Supplementary Figure S9). These findings demonstrate that Z5 not only effectively inhibits the growth of GSCs in vivo but is also sufficiently safe.

These collective findings establish Z5 as a potent EGFR inhibitor that exerts its anti-glioblastoma effects through a precisely orchestrated mechanism. Z5 initially targets and binds to the E762 residue of EGFR, which serves as the first step in initiating downstream molecular events. This interaction subsequently leads to the induction of DNA damage and impairs the cellular DNA repair machinery. Concurrently, Z5 disrupts the critical EGFR-WEE1 protein–protein interaction, further compromising the function of WEE1 — a key regulator of the G2/M checkpoint. The combined disruption of DNA repair and WEE1 signaling culminates

in mitotic catastrophe and tumor cell death (Figure 7G). The therapeutic potential of this multi-targeted mechanism is robustly demonstrated by Z5's strong anti-tumor activity across a range of experimental models, including GBM cell lines, patient-derived GSCs, and orthotopic GSC-derived xenografts in mice.

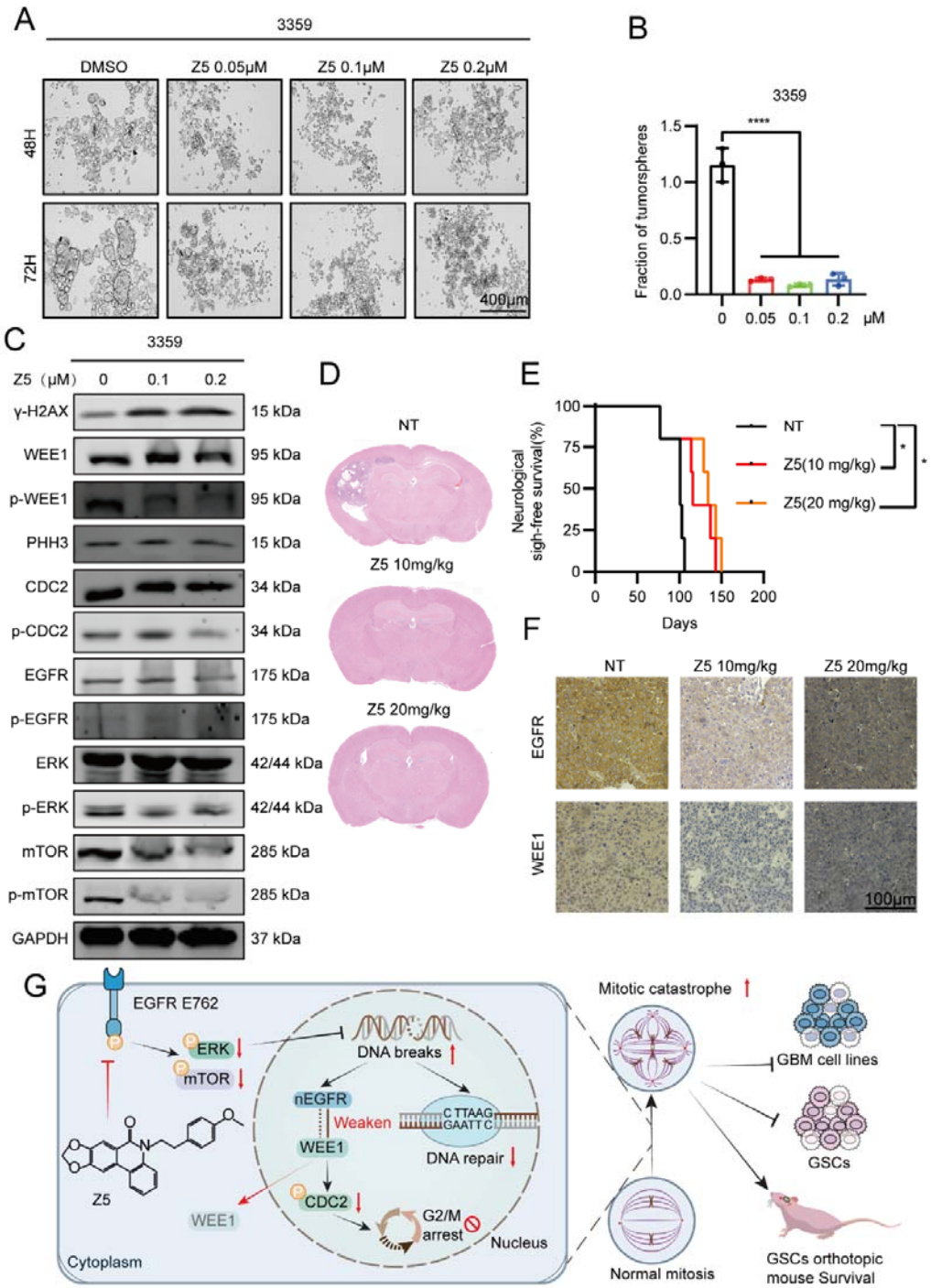

Figure 7 Z5 inhibits GSCs tumorigenesis and progression through EGFR-WEE1 axis disruption. (A) Microscopic observation of GSC-derived tumor sphere formation in 3359 cells after incubation with different concentrations of Z5 for 48 hours. (B) Quantitative analysis of the fragmentation of tumor spheres from (A). Data are

presented as the mean ± SD, n=3, ****p < 0.0001, compared with “0” group. (C) The expressions level of γ-H2AX, WEE1, p-WEE1, PHH3, CDC2, p-CDC2, EGFR, p-EGFR, ERK, p-ERK, mTOR, p-mTOR in 3359 treated with or without Z5. (D) H&E staining to evaluate intracranial tumor formation. (E) Survival analysis of mice with orthotopically transplanted GSCs. Data are presented as the mean ± SD, n=4, *p < 0.05, compared with NT group. (F) Immunohistochemistry examination of EGFR and WEE1 expression in orthotopic xenografts in mice. (G) Detailed molecular mechanisms of Z5-mediated anti-GBM effects through targeting EGFR and WEE1.

The ethical approval number: 2021-lEC-A244 and IACUC Number:3028

4. Discussion

Since TMZ's approval in 2005, despite extensive research, no transformative GBM therapies have emerged. While tumor-treating fields, molecularly targeted agents (e.g., EGFR/VEGF inhibitors), and immunotherapy have been integrated into clinical practice, their efficacy is limited by tumor heterogeneity, immunosuppressive microenvironment, and BBB exclusion, resulting in high recurrence rates (>90%)[32,33]. This unmet need drives our identification of Z5, a potent anti-GBM agent with demonstrated safety. We elucidated its mechanism as an EGFR inhibitor and validated its therapeutic efficacy.

Phenanthridinone-derived natural products have demonstrated promising anti-tumour properties through EGFR-related mechanisms. For instance, lycorine induces apoptosis in GBM cells via EGFR inhibition and exhibits favorable therapeutic efficacy in patient-derived GBM xenograft models[34]. Similarly, narciclasine suppresses gastric cancer cell proliferation by modulating the

AKT/mTOR signaling pathway[35] , while also functioning as a TOP1 inhibitor that induces G2/M phase arrest and promotes apoptosis in cancer cells[36]. Notably, narciclasine demonstrates remarkable therapeutic efficacy at low dosages—extending survival in orthotopic GBM mouse models at just 1 mg/kg[37,38]. These findings highlight the therapeutic potential of the phenanthridone scaffold, which may simultaneously engage EGFR targeting and DNA intercalation mechanisms. Importantly, Z5, as a representative of this scaffold, not only inherits these pharmacological features but also demonstrates potent anti-GBM efficacy.

Conventional EGFR inhibitors (gefitinib, osimertinib) show limited GBM efficacy due to tumor heterogeneity, redundant pathways, and BBB penetration challenges[15,39,40]. Our studies reveal Z5's unique approach: direct binding to EGFR's E762 residue disrupts its kinase activity while subsequently inducing conformational changes that prevent EGFR-WEE1 interaction. This effect addresses two critical vulnerabilities in GBM—aberrant EGFR signaling and compromised cell cycle checkpoint control. Unlike nuclear EGFR targeting strategies that focus on downstream oncogene upregulation[41,42], Z5's mechanism combines immediate kinase inhibition with sustained disruption of DNA repair pathways through WEE1 modulation. This is particularly relevant as GBM cells rely on EGFR amplification to drive proliferation and radiation resistance while depending on WEE1 to survive replication stress.

Using single-molecule magnetic tweezers and cell models, we previously confirmed that Z5 is a DNA intercalator[22]. DNA intercalators reversibly bind to

double-stranded DNA (dsDNA) through non-covalent interactions—such as van der Waals forces, hydrogen bonds, hydrophobic effects, and charge-transfer interactions—causing structural changes that affect DNA stability and its interaction with proteins Unlike alkylating agents, which cause irreversible DNA damage via covalent bonding, intercalators must first form a relatively stable complex with DNA to exert cytotoxic effects. These complexes can interfere with DNA replication, transcription, and repair by disrupting the function of DNA-associated enzymes[43-45]. Unlike alkylating agents, which cause irreversible DNA damage via covalent bonding, intercalators must first form a relatively stable complex with DNA to exert cytotoxic effects. These complexes can interfere with DNA replication, transcription, and repair by disrupting the function of DNA-associated enzymes. Anthracyclines like doxorubicin are classic examples; although they intercalate into DNA, their main cytotoxic effect comes from topoisomerase II inhibition, leading to DNA breaks and cell death. Compared to strong intercalators such as YOYO-1 and ethidium bromide, Z5 exhibits moderate intercalation strength. This suggests it may have lower mutagenic and carcinogenic risks. Indeed, toxicity studies in various normal cells and animal models have shown that Z5 has low cytotoxicity[22]. In this study, long-term toxicity assessment (over 150 days) in a GSC-derived orthotopic GBM mouse model further supported this finding.

Our investigation reveals that Z5 exerts its anti-GBM effects through a multifaceted mechanism targeting EGFR. Specifically, Z5 initially binds to the E762 residue within the kinase domain of EGFR, which leads to subsequent induction of DNA double-strand breaks (DSBs). This is followed by disruption of the critical interaction

between EGFR and WEE1. This sequential mode of action aligns with the molecular pathology of GBM. The therapeutic rationale for Z5 is further strengthened by WEE1's critical role in cancer biology. As a key cell-cycle checkpoint kinase, WEE1 phosphorylates CDK1/2 to enforce G2/M arrest, allowing time for DNA repair before mitosis. In cancer cells, WEE1 overexpression correlates with poor prognosis and therapeutic resistance, while its inhibition forces mitotic catastrophe in genomically unstable cells[46]. Given that GBM cells critically depend on WEE1 to survive replication stress induced by EGFR amplification and radiation therapy, Z5's ability to simultaneously target EGFR and disrupt WEE1-mediated checkpoint control provides a mechanistically sound and clinically compelling therapeutic approach.

Our study has several limitations. Although functional crosstalk between EGFR and WEE1 in DNA damage response is established, the structural basis of their interaction remains poorly defined [7,47,48]. Our data demonstrate that Z5 binding to EGFR's E762 residue disrupts their association, but the precise binding interface - including whether WEE1 engages EGFR through single or multiple contact points - remains to be elucidated. Additionally, the conformational changes induced by Z5 at E762 and their direct impact on WEE1's kinase activity require structural validation through co-crystallization studies. The temporal relationship between EGFR inhibition, WEE1 disruption, and DNA damage induction also warrants clarification. Comparative studies in other cancers provide intriguing insights: while combined EGFR and WEE1 inhibition shows limited efficacy in esophageal squamous cell carcinoma (ESCC) [49], synergistic effects have been observed in leptomeningeal carcinomatosis models[50].

These observations underscore the complexity of EGFR-WEE1 interactions across different cancer types and highlight the need for cancer-specific therapeutic strategies.

In conclusion, Z5's unique mechanism—initiating EGFR targeting at the E762 residue, which sequentially induces DNA damage, disrupts EGFR-WEE1 interaction, and compromises DNA repair pathways—offers a paradigm shift in GBM therapy by simultaneously addressing two critical vulnerabilities: aberrant proliferation signaling and genomic instability. Our work establishes a framework for phenanthridone derivatives as multi-mechanistic anti-GBM agents, warranting further clinical translation.

Availability of Data and Materials

This study did not generate new regents or original code. All data generated or analyzed during this study are included in this article and its supplementary information files. Microarray data can be accessed through the following link: https://ngdc.cncb.ac.cn/omix/preview/BlYvj2iS.

5. References

1 Weller M, Wen PY, Chang SM, Dirven L, Lim M, Monje M, et al. Glioma. *Nature Reviews Disease Primers* 2024;**10**:33.

2 Grochans S, Cybulska AM, Simińska D, Korbecki J, Kojder K, Chlubek D, et al. Epidemiology of Glioblastoma Multiforme-Literature Review. *Cancers* 2022;**14**.

3 Alick P WJJ. A Review of Glioblastoma and Other Primary Brain Malignancies. 2023;**330**.

4 Rodriguez SMB, Kamel A, Ciubotaru GV, Onose G, Sevastre AS, Sfredel V, et al. An Overview of EGFR Mechanisms and Their Implications in Targeted Therapies for Glioblastoma. *Int J Mol Sci* 2023;**24**.

5 Lin B, Ziebro J, Smithberger E, Skinner KR, Zhao E, Cloughesy TF, et al. EGFR, the Lazarus target for precision oncology in glioblastoma. *Neuro Oncol* 2022;**24**:2035-62.

6 Liccardi G, Hartley JA, Hochhauser D. EGFR nuclear translocation modulates DNA repair following cisplatin and ionizing radiation treatment. *Cancer Res* 2011;**71**:1103-14.

7 Zhou Z, Lu H, Zhu S, Gomaa A, Chen Z, Yan J, et al. Activation of EGFR-DNA-PKcs pathway by IGFBP2 protects esophageal adenocarcinoma cells from acidic bile salts-induced DNA damage. *J Exp Clin Cancer Res* 2019;**38**:13.

8 Meyn RE, Munshi A, Haymach JV, Milas L, Ang KK. Receptor signaling as a regulatory mechanism of DNA repair. *Radiother Oncol* 2009;**92**:316-22.

9 Rajput M, Singh R, Singh N, Singh RP. EGFR-mediated Rad51 expression potentiates intrinsic resistance in prostate cancer via EMT and DNA repair pathways. *Life Sci* 2021;**286**:120031.

10 Prewett M, Deevi DS, Bassi R, Fan F, Ellis LM, Hicklin DJ, et al. Tumors established with cell lines selected for oxaliplatin resistance respond to oxaliplatin if combined with cetuximab. *Clin Cancer Res* 2007;**13**:7432-40.

11 Justin T, Nishika K, Jian L C. Therapeutic Targets in Glioblastoma: Molecular Pathways, Emerging Strategies, and Future Directions. *Cells* 2025;**14**.

12 Chen Z, Vallega KA, Wang D, Quan Z, Fan S, Wang Q, et al. DNA topoisomerase II inhibition potentiates osimertinib's therapeutic efficacy in EGFR-mutant non-small cell lung cancer models. *J Clin Invest* 2024;**134**.

13 Lee MJ, Ye AS, Gardino AK, Heijink AM, Sorger PK, MacBeath G, et al. Sequential application of anticancer drugs enhances cell death by rewiring apoptotic signaling networks. *Cell* 2012;**149**:780-94.

14 An Z, Aksoy O, Zheng T, Fan QW, Weiss WA. Epidermal growth factor receptor and EGFRvIII in glioblastoma: signaling pathways and targeted therapies. *Oncogene* 2018;**37**:1561-75.

15 Li X-P, Guo Z-Q, Wang B-F, Zhao M. EGFR alterations in glioblastoma play a role in antitumor immunity reg ulation. *Front Oncol*;**13**.

16 Jin Z, Yao G. Amaryllidaceae and Sceletium alkaloids. *Natural Product Reports* 2019.

17 Azad I, Ahmad R, Khan T, Saquib M, Hassan F, Akhter Y, et al. Phenanthridine derivatives as promising new anticancer agents: synthesis, biological evaluation and binding studies. *Future medicinal chemistry* 2020;**12**:709-39.

18 Ingrassia L, Lefranc F, Dewelle J, Pottier L, Mathieu V, Spiegl-Kreinecker S, et al. Structure−activity relationship analysis of novel derivatives of narciclasine (an Amaryllidaceae isocarbostyril derivative) as potential anticancer agents. *Journal of Medicinal Chemistry* 2009;**52**:1100-14.

19 Van Goietsenoven G, Mathieu V, Lefranc F, Kornienko A, Evidente A, Kiss R. Narciclasine as well as other Amaryllidaceae Isocarbostyrils are Promising GTP-ase Targeting Agents against Brain Cancers. *Medicinal research reviews* 2013;**33**:439-55.

20 F ü rst RJPm. Narciclasine – an amaryllidaceae alkaloid with potent antitumor and anti-inflammatory properties. *Planta medica* 2016;**82**:1389-94.

21 Yuan M, Chen L, Wang J, Chen S, Wang K, Xue Y, et al. Transition-metal-free synthesis of phenanthridinones from biaryl-2-oxamic acid under radical conditions. *Organic Letters* 2015;**17**:346-9.

22 Tong Q, You H, Chen X, Wang K, Sun W, Pei Y, et al. ZYH005, a novel DNA intercalator, overcomes all-trans retinoic acid resistance in acute promyelocytic leukemia. *Nucleic Acids*

Res 2018;**46**:3284-97.

23 Liu D, Zhu H, Cheng L, Li R, Ma X, Wang J, et al. Hypoxia-induced galectin-8 maintains stemness in glioma stem cells via autophagy regulation. *Neuro Oncol* 2024;**26**:872-88.

24 Wu X, Takenaka K, Sonoda E, Hochegger H, Kawanishi S, Kawamoto T, et al. Critical roles for polymerase zeta in cellular tolerance to nitric oxide-induced DNA damage. *Cancer Res* 2006;**66**:748-54.

25 Beyett TS, Rana JK, Schaeffner IK, Heppner DE, Eck MJ. Structural Analysis of the Macrocyclic Inhibitor BI-4020 Binding to EGFR Kinase. *ChemMedChem* 2024;**19**:e202300343.

26 Unni S, Huang Y, Hanson RM, Tobias M, Krishnan S, Li WW, et al. Web servers and services for electrostatics calculations with APBS and PDB2PQR. *J Comput Chem* 2011;**32**:1488-91.

27 Morris GM, Huey R, Lindstrom W, Sanner MF, Belew RK, Goodsell DS, et al. AutoDock4 and AutoDockTools4: Automated docking with selective receptor flexibility. *J Comput Chem* 2009;**30**:2785-91.

28 Malinovska L, Cappelletti V, Kohler D, Piazza I, Tsai TH, Pepelnjak M, et al. Proteome-wide structural changes measured with limited proteolysis-mass spectrometry: an advanced protocol for high-throughput applications. *Nat Protoc* 2023;**18**:659-82.

29 Lamb J, Crawford ED, Peck D, Modell JW, Blat IC, Wrobel MJ, et al. The Connectivity Map: using gene-expression signatures to connect small molecules, genes, and disease. *Science* 2006;**313**:1929-35.

30 Gimple RC, Bhargava S, Dixit D, JN R. Glioblastoma stem cells: lessons from the tumor hierarchy in a lethal cancer. *Genes Dev* 2019;**33(11-12)**:591-609.

31 Suva ML, Tirosh I. The Glioma Stem Cell Model in the Era of Single-Cell Genomics. *Cancer Cell* 2020;**37**:630-6.

32 Liu Y, Zhou F, Ali H, Lathia JD, Chen P. Immunotherapy for glioblastoma: current state, challenges, and future perspectives. *Cellular & Molecular Immunology* 2024;**21**:1354-75.

33 Davis ME. Glioblastoma: Overview of Disease and Treatment. *Clinical journal of oncology nursing* 2016;**20**:S2-8.

34 Shen J, Zhang T, Cheng Z, Zhu N, Wang H, Lin L, et al. Lycorine inhibits glioblastoma multiforme growth through EGFR suppression. *J Exp Clin Cancer Res* 2018;**37**:157.

35 Yuan Y, He X, Li X, Liu Y, Tang Y, Deng H, et al. Narciclasine induces autophagy-mediated apoptosis in gastric cancer cells through the Akt/mTOR signaling pathway. *BMC Pharmacol Toxicol* 2021;**22**:70.

36 Wang M, Liang L, Wang R, Jia S, Xu C, Wang Y, et al. Narciclasine, a novel topoisomerase I inhibitor, exhibited potent anti-cancer activity against cancer cells. *Nat Prod Bioprospect* 2023;**13**:27.

37 Lefranc F, Sauvage S, Van Goietsenoven G, Megalizzi V, Lamoral-Theys D, Debeir O, et al. Narciclasine, a plant growth modulator, activates Rho and stress fibers in glioblastoma cells. *Mol Cancer Ther* 2009;**8**:1739-50.

38 Van Goietsenoven G, Mathieu V, Lefranc F, Kornienko A, Evidente A, Kiss R. Narciclasine as well as other Amaryllidaceae isocarbostyrils are promising GTP-ase targeting agents against brain cancers. *Med Res Rev* 2013;**33**:439-55.

39 Lee A, Arasaratnam M, Chan DLH, Khasraw M, Howell VM, Wheeler H. Anti-epidermal growth factor receptor therapy for glioblastoma in adults. *The Cochrane database of*

systematic reviews 2020;**5**:Cd013238.

40 Westphal M, Maire CL, Lamszus K. EGFR as a Target for Glioblastoma Treatment: An Unfulfilled Promise. *CNS Drugs* 2017;**31**:723-35.

41 Lo HW, Hung MC. Nuclear EGFR signalling network in cancers: linking EGFR pathway to cell cycle progression, nitric oxide pathway and patient survival. *Br J Cancer* 2006;**94**:184-8.

42 Brand TM, Iida M, Luthar N, Starr MM, Huppert EJ, Wheeler DL. Nuclear EGFR as a molecular target in cancer. *Radiother Oncol* 2013;**108**:370-7.

43 Martinez R, Chacón-García. L. The search of DNA-intercalators as antitumoral drugs: what it worked and what did not work. *Current Medicinal Chemistry* 2005;**12**:127-51.

44 Venugopal S, Sharma V, Mehra A, Singh I, Singh G. DNA intercalators as anticancer agents. *Chem Biol Drug Des* 2022;**100**:580-98.

45 Biebricher AS, Heller I, Roijmans RFH, Hoekstra TP, Peterman EJG, Wuite GJL. The impact of DNA intercalators on DNA and DNA-processing enzymes elucidated through force-dependent binding kinetics. *Nature communications* 2015;**6**:7304.

46 Ghelli Luserna di Rorà A, Cerchione C, Martinelli G, Simonetti G. A WEE1 family business: regulation of mitosis, cancer progression, and therapeutic target. *Journal of hematology & oncology* 2020;**13**:126.

47 Cetin MH, Rieckmann T, Hoffer K, Riepen B, Christiansen S, Gatzemeier F, et al. G2 checkpoint targeting via Wee1 inhibition radiosensitizes EGFRvIII-positive glioblastoma cells. *Radiat Oncol* 2023;**18**:19.

48 Volman Y, Hefetz R, Galun E, Rachmilewitz J. DNA damage alters EGFR signaling and reprograms cellular response via Mre-11. *Sci Rep* 2022;**12**:5760.

49 Chen D, Hong R, Cao Y, Wu Q, Wang Y, Chen J, et al. Combined Wee1 and EGFR inhibition reveals synergistic antitumor effect in esophageal squamous cell carcinoma. *Carcinogenesis* 2023;**44**:451-62.

50 Fukuda K, Nanjo S, Takeuchi S, Chakrabarti T, Brown T, Dev Sahadevan SW, et al. Targeting WEE1 to overcome ARID1A mutation-driven osimertinib resistance in EGFR-mutant lung cancer. *J Thorac Oncol* 2025.

775